Sustainable Oxidative Cleavage of Vegetable Oils into Diacids by Organo-Modified Molybdenum Oxide Heterogeneous Catalysts

Aimé Serge Ello, Amir Enferadi-kerenkan, Albert Trokourey & Trong-On Do

Journal of the American Oil Chemists' Society

ISSN 0003-021X
Volume 94
Number 12

J Am Oil Chem Soc (2017) 94:1451-1461
DOI 10.1007/s11746-017-3047-2

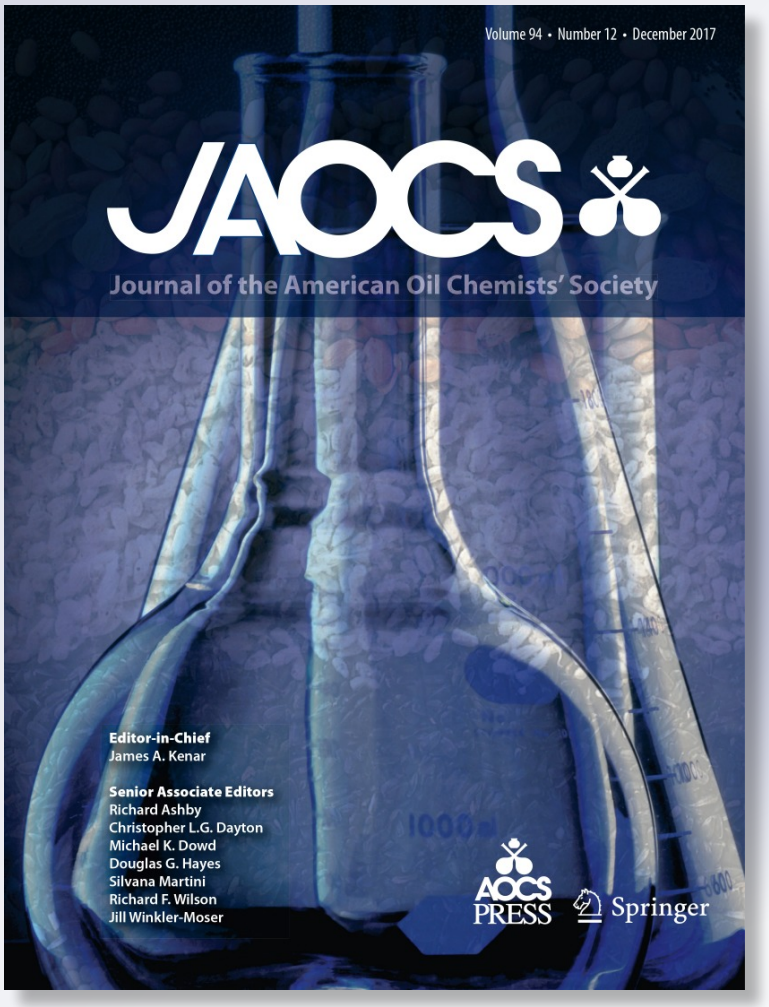

Springer

J Am Oil Chem Soc (2017) 94:1451–1461
DOI 10.1007/s11746-017-3047-2

ORIGINAL PAPER

Sustainable Oxidative Cleavage of Vegetable Oils into Diacids by Organo-Modified Molybdenum Oxide Heterogeneous Catalysts

Aimé Serge Ello[1,2] · Amir Enferadi-kerenkan[1] · Albert Trokourey[2] · Trong-On Do[1]

Received: 26 June 2017 / Revised: 28 August 2017 / Accepted: 7 September 2017 / Published online: 21 September 2017

Abstract Exploiting vegetable oils to produce industrially valuable diacids via an eco-friendly process requires an efficient and recyclable catalyst. In this work, a novel catalytic system based on organo-modified molybdenum trioxide was synthesized by a green hydrothermal method in one simple step, using Mo powder as precursor, hydrogen peroxide, and amphiphilic surfactants cetyltrimethylammonium bromide (CTAB) and tetramethylammonium bromide (TMAB) as capping agents. The synthesized materials were first characterized by different techniques including XRD, SEM, TGA, and FT-IR. Interestingly, various morphologies were obtained depending on the nature of the surfactants and synthetic conditions. The synthesized catalysts were employed in oxidative cleavage of oleic acid, the most abundant unsaturated fatty acid, to produce azelaic and pelargonic acids with a benign oxidant, H_2O_2. Excellent catalytic activities resulting in full conversion of initial oleic acid were obtained, particularly for CTAB-capped molybdenum oxide (CTAB/Mo molar ratio of 1:3) that gave 83 and 68% yields of production of azelaic and pelargonic acids, respectively. These are the highest yields that have been obtained for this reaction by heterogeneous catalysts up to now. Moreover, the CTAB-capped catalyst could be conveniently separated from the reaction mixture by simple centrifugation and reused without significant loss of activity up to at least four cycles.

Keywords Oleic acid · Oxidative cleavage · Azelaic acid · Surfactant · Molybdenum oxide · Heterogeneous catalysis

Introduction

Biomass-derived feedstock is one of the most promising candidates that would substitute the crude oil-based fuels and chemicals. The vast abundance and renewable nature of vegetable oils have attracted growing interest in both academic and industrial researches. Triglyceride is the main component of oleaginous feedstock, i.e. vegetable oils, of which its unsaturated fatty acids can be chemically modified, mainly through their double bonds, to be converted into value-added chemicals. For instance, oleic acid, the most abundant monounsaturated fatty acid [1], can produce di- and mono-carboxylic, azelaic and pelargonic acids through oxidative cleavage reaction, which are valuable materials for different industrial applications like production of polymers, plasticizers, adhesives, lubricants, cosmetics, herbicides, and fungicides, etc. [2–6]. Currently, the oxidative cleavage of oleic acid is performed in industry via ozonolysis. However, using ozone is not in line with the principles of sustainable chemistry due to its inevitable hazardous problems. Attempting to employ a benign oxidant, several catalyst/oxidant systems, in homogeneous and heterogeneous forms, have been reported in the literature for oxidative cleavage of unsaturated fatty acids, which have been thoroughly reviewed in our recent review paper [7].

Electronic supplementary material The online version of this article (doi:10.1007/s11746-017-3047-2) contains supplementary material, which is available to authorized users.

Aimé Serge Ello and Amir Enferadi-kerenkan contributed equally to this work.

✉ Trong-On Do
trong-on.do@gch.ulaval.ca

[1] Department of Chemical Engineering, Laval University, Quebec G1V 0A6, Canada

[2] Laboratoire de Chimie Physique, Université Félix Houphouët-Boigny de Cocody, 22 bp 582 Abidjan, Côte d'Ivoire

Homogeneous catalysts have generally shown excellent performances in oxidation of unsaturated fatty acids (e.g. production yield of azelaic acid up to 82% from oleic acid by peroxo complex, oxoperoxo (pyridine-2,6-dicarboxylato) molybdenum (VI) hydrate {$Mo(O_2)[C_5H_3N(CO_2)_2](H_2O)$} catalysts [6]), but such catalytic systems have always been associated with a lack of catalyst recovery. On the other hand, activities of heterogeneous catalysts, with recoverability, reported so far, are not as high as homogeneous ones [7, 8]. Various strategies have been reported in the literature to improve the efficiency of the reaction, like reaction in supercritical fluids with dual oxidants and microwave irradiations and ultrasound-assisted reactions [9–12]. Works should be encouraged to find a suitable reaction strategy that enjoys both high activity and efficient recovery. Current efforts in this domain can be generally classified into two groups. The first group is involving different transition metal oxide catalysts, which are inherently solid, along with a benign oxidant such as hydrogen peroxide or sodium hypochlorite, and the second group is based on heterogenization of highly active homogeneous catalysts, like polyoxometallates, via immobilization or solidification methods [13–16]. In these two groups, direct or indirect selective oxidative cleavage mechanisms have been proposed [17]. Nevertheless, an efficient heterogeneous catalytic system that can afford the excellent reaction yields obtained by the homogeneous catalysts has not been reported so far.

In this work, we have tried to push the proved potential of molybdenum oxide as an oxidizing solid catalyst [18–20] to oxidative cleavage reaction of unsaturated fatty acids. Curiously, employing MoO_3 heterogeneous catalysts in oxidative cleavage of oleic acid has not been reported so far, to our knowledge. Herein, a series of molybdenum oxides were synthesized via simple oxidative dissolution of Mo powder in H_2O_2, with and without organic surfactants. Two well-known quaternary ammonium surfactants, cetyltrimethylammonium bromide (CTAB) and tetramethylammonium bromide (TMAB) with different alkyl chain lengths were employed as capping agents. Effects of CTAB and TMAB with different concentrations in the synthesis medium on physicochemical properties and morphology of the products, as well as enhancement of catalytic efficiency in the liquid phase oxidative cleavage of oleic acid by organo-modification of the surface of molybdenum oxide have been investigated.

Experimental

Synthetic Details

Surfactant-capped molybdenum oxide particles were synthesized by hydrothermal method using molybdenum powder (99.9%, Alfa Aesar), hydrogen peroxide (30%, Fischer Scientific), and surfactants; CTAB (98%, Fischer Scientific) and TMAB (98%, Aldrich). In a typical synthesis, 1 g of metallic molybdenum powder was added to 10 ml of deionized water and the mixture was stirred for 30 min at room temperature. Then, the mixture was placed in an ice bath under a well-ventilated fume hood. To this mixture, an aqueous solution of hydrogen peroxide was added dropwise under vigorous stirring until the color of the solution changed to yellow (attention: the reaction is very exothermic and must be done in an ice bath under skilled supervision). The determined amounts of surfactants (CTAB or TMAB) to obtain surfactant/molybdenum molar ratios of 1:2, 1:3, and 1:4 were added to the yellow solution. The resultant slurry was refluxed at 100 °C for 4 h. Finally, the solid product was separated by centrifugation at high speed and dried in air at 70 °C for 10 h.

Characterization Equipment

The physicochemical properties of the materials were characterized by X-ray diffraction (XRD), scanning electron microscopy (SEM), thermogravimetric analysis (TGA), and Fourier transform infrared spectroscopy (FT-IR). Powder XRD patterns of the samples were obtained on a Bruker SMART APEXII X-ray diffractometer equipped with a Cu Kα radiation source ($\lambda = 1.5418$ Å) with steps of 0.02^0 and step time of 1 s. SEM images were taken on a JEOL 6360 instrument at an accelerating voltage of 3 kV. Materials were spread on a carbon tape prior to analysis. The FT-IR spectra were recorded on an FTS 45 infrared spectrophotometer with the KBr pellet technique. TGA was performed in the temperature range of 30–800 °C with a TGA Q500 V20.13 Build 39 thermogravimetric analyzer at a heating rate of 5 °C min^{-1} under an air flow or argon flow of 50 ml min^{-1}.

Catalytic Test

Catalytic reactions were carried out in a glass reactor equipped with an oil bath, magnetic stirrer, and reflux condenser. Typically, the reactor was charged with a suspension of 0.4 g catalyst and 4 ml aqueous H_2O_2. Then, 1 g oleic acid (≥99%, Sigma-Aldrich) was added dropwise under stirring followed by addition of 8 ml of *tert*-butanol as solvent. The reaction mixture was heated to 85 °C and kept at this temperature for a reaction time of 3 h 30 min. After the reaction, the solution was allowed to cool to room temperature. During the reaction, the system showed homogeneous catalysis properties, while upon cooling at the end of reaction, the catalyst particles were precipitated, enabling self-separation. The precipitated catalyst was separated using a centrifuge at 8000 rpm and recovered via washing with ethanol and water several times and drying at 70 °C for 4 h, in order to be

used in the next catalytic cycle. The resultant solution then underwent a derivatization process prior to gas chromatography–mass spectrometry (GC–MS) analysis.

Quantitative Analysis of the Product

GC–MS was used for separation and quantification of methyl esters of fatty acids. Since fatty acids in their free forms are difficult to analyze with GC (due to their adsorption issues on stationary phase in GC columns), the reaction products were esterified before GC–MS analysis via Metcalfe *et al*. derivatization procedure [21, 22] using boron trifluoride solution in methanol. Briefly, BF_3-methanol (5 ml; 10% w/w, Sigma-Aldrich Co.) was added to the solution of products of the oxidation reaction. Then, the solution was heated to 80 °C for 15 min, followed by cooling at room temperature for about 20 min. The esterified products were extracted by adding 3 ml of petroleum ether and 2 ml of water. The extraction was repeated for the aqueous phase (lower layer) twice. Obtained organic phase, after dehydration by sodium sulfate and removal of the solvent by passing a steady stream of dry air, was ready for injection into the GC–MS instrument.

A typical derivatized sample including methyl esters of the involved fatty acids (expectedly dimethyl azelate, methyl pelargonate, and possibly methyl oleate) was injected into the GC–MS instrument which had been previously calibrated by analytical standards of these methyl esters. The GC–MS system included a Hewlett-Packard HP 5890 series GC system and an MSD Hewlett-Packard model 5970. The GC system was equipped with Zebron ZB-5MS capillary column (30 m × 0.25 mm × 0.25 mm). Helium was used as a carrier gas with the flow rate of 30 ml/min. A split ratio of 15:1 was fixed. The front inlet temperature was 280 °C. The oven temperature program consisted of maintaining at 50 °C for 2 min, then a ramp rate of 10 °C/min to 160 °C following by a hold-up time of 1 min, and further increase of the rate of 5 °C/min to 290 °C. Direct injection was employed with a 1-µl injection amount for each run, and the injection was repeated at least four times for each sample to be averaged. HP Chemstation software was used to analyze data.

Results and Discussion

Characterization of the Catalysts

Crystalline structures of the synthesized samples were analyzed by XRD. Figure 1 represents the XRD patterns of the synthesized molybdenum oxides. Presence of sharp peaks indicates good crystallinity of the products, which were synthesized even without using an autoclave and in a short time. The XRD pattern of the sample prepared without using any surfactant, denoted as MO (Fig. 1a), confirmed that it was composed of MoO_3–H_2O, in accordance with PDF no. 26-1449 of the ICDD library of spectra. The pattern exhibits five well-resolved peaks indexed to the (010), (100), (120), (020), and (030) planes of triclinic molybdenum trioxide hydrate material, and no peaks corresponding to other phases implies the single triclinic phase of this material.

Presence of surfactants CTAB and TMAB in the synthesis medium dramatically influenced the crystalline phase of molybdenum oxide. Figure 1b, c show XRD patterns of the samples prepared in the presence of these two surfactants with the surfactant/molybdenum molar ratio of 1:2 (denoted as MO–TMAB 1:2 and MO–CTAB 1:2). The XRD pattern of MO–TMAB (Fig. 1b) indicated that the quaternary ammonium cation could incorporate well into the crystalline structure of the final product. TMAB, also, affected the oxidation state of the formed molybdenum oxide. The peaks could be precisely indexed on monoclinic tetramethylammonium tetramolybdate, $[N(CH_3)_4]Mo_4O_{12}$ (PDF no. 50-1901), and ammonium octamolybdate tetrahydrate $(NH_4)_6Mo_8O_{27}{\cdot}4H_2O$ (PDF no. 50-0607). The surfactant with a longer organic chain, CTAB, directed the crystalline phase toward a multiphase structure. As seen in Fig. 1c, it has many more peaks than the previous samples in 2θ less than 15°, which could be mainly ascribed to the crystalline phases of MoO_3 (PDF no. 21-0569), ammonium molybdenum oxide hydrates $(NH_4)_6Mo_7O_{24}{\cdot}4H_2O$ (PDF no. 11-0071) and $(NH_4)_4(Mo_8O_{24.8}(O_2)_{1.2}(H_2O)_2)(H_2O)_4$ (PDF no. 88-1326), and tetramethylammonium tetramolybdate $[N(CH_3)_4]Mo_4O_{12}$ (PDF no. 50-1901). This multiphase is probably due to the cationic nature of CTAB during the synthesis reaction, which could be adsorbed by molybdenum oxide nuclei and afterward it would detach at different times to form multiple phases.

Figure 2 shows SEM images of the synthesized materials prepared with and without the surfactants. Apart from 1:2, two other molar ratios of surfactant/molybdenum (1:3 and 1:4) were used in the synthesis to investigate effects of the surfactants amounts on final morphology. The prepared samples are denoted as MO–CTAB 1:4, MO–CTAB 1:3, MO–TMAB 1:4, and MO–TMAB 1:3. The SEM image of MO, synthesized without surfactant (Fig. 2a), demonstrates one-dimensional nanorods of a few micrometers in length.

Obviously, different sizes and morphologies were observed according to concentration as well as nature of the surfactant used (Fig. 2b–g). A lower amount of CTAB in MO–CTAB 1:4 (Fig. 2b) did not change the morphology significantly; similar nanorods were obtained. Increasing CTAB content in MO–CTAB 1:3, however, a heterogeneous mixture of nanorods and microplatelet-like morphology was obtained (Fig. 2c), which became homogeneous microplatelets in MO–CTAB 1:2. The effect of a high concentration of CTAB is in good agreement with the previous works, where

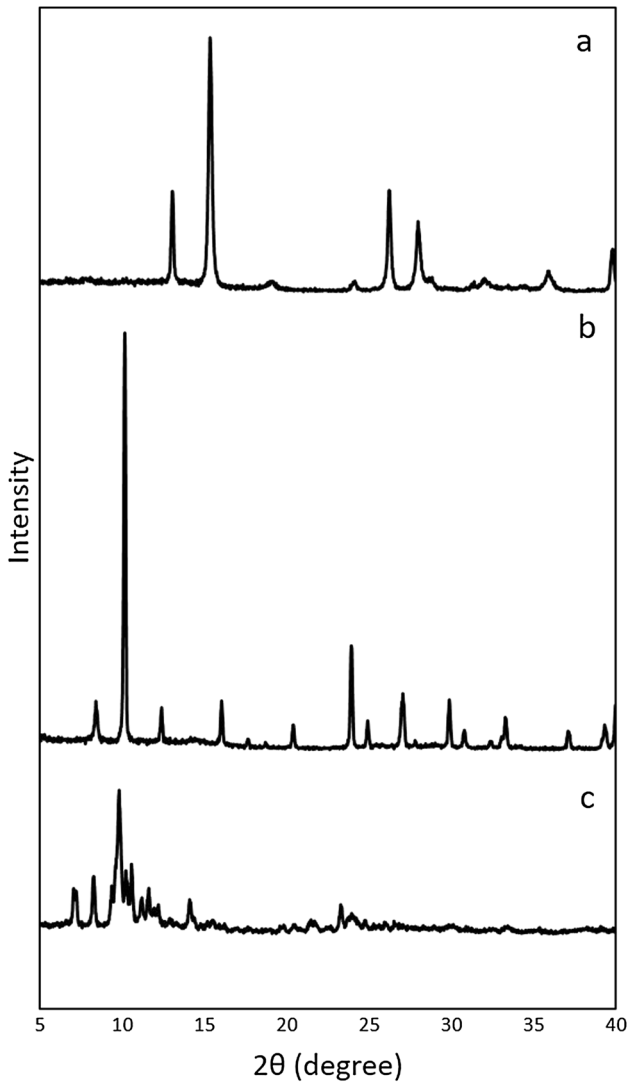

Fig. 1 XRD patterns of the synthesized molybdenum oxides: **a** MO (without surfactant), **b** MO–TMAB 1:2, and **c** MO–CTAB 1:2

a stacked micro-size of MoO_3 fibers and a micro-ellipsoid structure of MoO_3 were predominant [23, 24].

Using TMAB in the synthesis considerably increased the size of the product particles, leading to a heterogeneous mixture of microrods, which turned to agglomerated rods when the concentration of was TMAB increased (Fig. 2e–g). By contrast to CTAB, the size of these hybrid particles containing TMAB did not change considerably by changing the amount of TMAB. From these studies, it can be observed that morphology of the particles has been influenced significantly by the nature of the surfactants.

Generally, the mechanism of MoO_3 formation follows the anisotropic growing of MoO_6 octahedral crystal nuclei as a basic building unit of MoO_3 [25, 26]. In the absence of any surfactant in the synthesis medium, the growth along the [010] direction is much more favored, and thus, results in formation of nanofiber, as shown in Fig. 2a. Although using a low amount of CTAB in MO–CTAB 1:4 did not significantly change the morphology (Fig. 2b), a further increase of CTAB in MO–CTAB 1:3 and MO–CTAB 1:2 led to formation of an emulsion, highly likely because the concentration of CTAB reached the critical micelle concentration (CMC). The lipophilic groups of micelles tend to move inward and hydrophobic groups outward. The concentration of CTAB up to 1:3 led to a stable spherical micelle and still generated thin fibers. However, the further increase of CTAB concentration beyond the CMC increased the deformation of micelles [25]. It has been reported that at higher concentrations of CTAB, the shape of micelles changes from a sphere to a prolate ellipsoid, and then the preferred orientation growth of MoO_3 is inhibited, resulting in the micro-ellipsoid structure [25]. The concentration of CTAB up to 1:3 led to both spherical and deformed micelles; thus, the material possesses both a fiber and a plate morphology in Fig. 2c. The highest concentration of CTAB generated homogeneous deformed micelles, leading to only large plates in MO–CTAB 1:2 (Fig. 2b). The use of TMAB as a surfactant apparently could not produce enough micelles, and the concentration of TMAB appears to have no effect on the size of particles. According to the literature, the Ostwald ripening mechanism [27] leads to the formation of hexagonal rods after growth, and TMAB has not shown much effect; this was confirmed by XRD analysis (Fig. 1c).

FT-IR analysis has been employed to identify the presence of surface functional groups on the catalyst. Figures 3 and 4 show the FT-IR spectra of the samples prepared with CTAB and TMAB, respectively. In both figures, FT-IR spectra of the corresponding surfactant, as well as the MO sample (prepared without surfactant), have been also included to gain better interpretations.

Figure 3 shows two bands at 2920 and 2850 cm^{-1} for the CTAB-containing samples (Fig. 3a–c), which are attributed to the characteristic peaks of symmetric and asymmetric C–H stretching vibrations of methylene groups of CTAB. Moreover, the characteristic peak of angular deformation vibrations of a methylene group was also observed at 1475 cm^{-1} in these samples. These results were verified by the spectrum of pure CTAB (Fig. 3e).

As seen in Fig. 4, asymmetric and symmetric deformation modes pertaining to $(CH_3)_3N^+$ of the head group of TMAB appear at around 1490 and 1390 cm^{-1}, according to the literature [23]. A pure TMAB spectrum (Fig. 4e) shows the deformation vibrations of methyl groups at 1490 and 1397 cm^{-1} and all other samples containing TMAB confirm these characteristic peaks (Fig. 4a–c). Detailed analysis of the spectrum of the MO sample (Figs. 3d or 4d) reveals that the characteristic peak of stretching vibrations of Mo–O appears at 540 cm^{-1} [23, 27, 28], which was shifted to 563 and 556 cm^{-1} in the presence of CTAB and to 580 cm^{-1} in

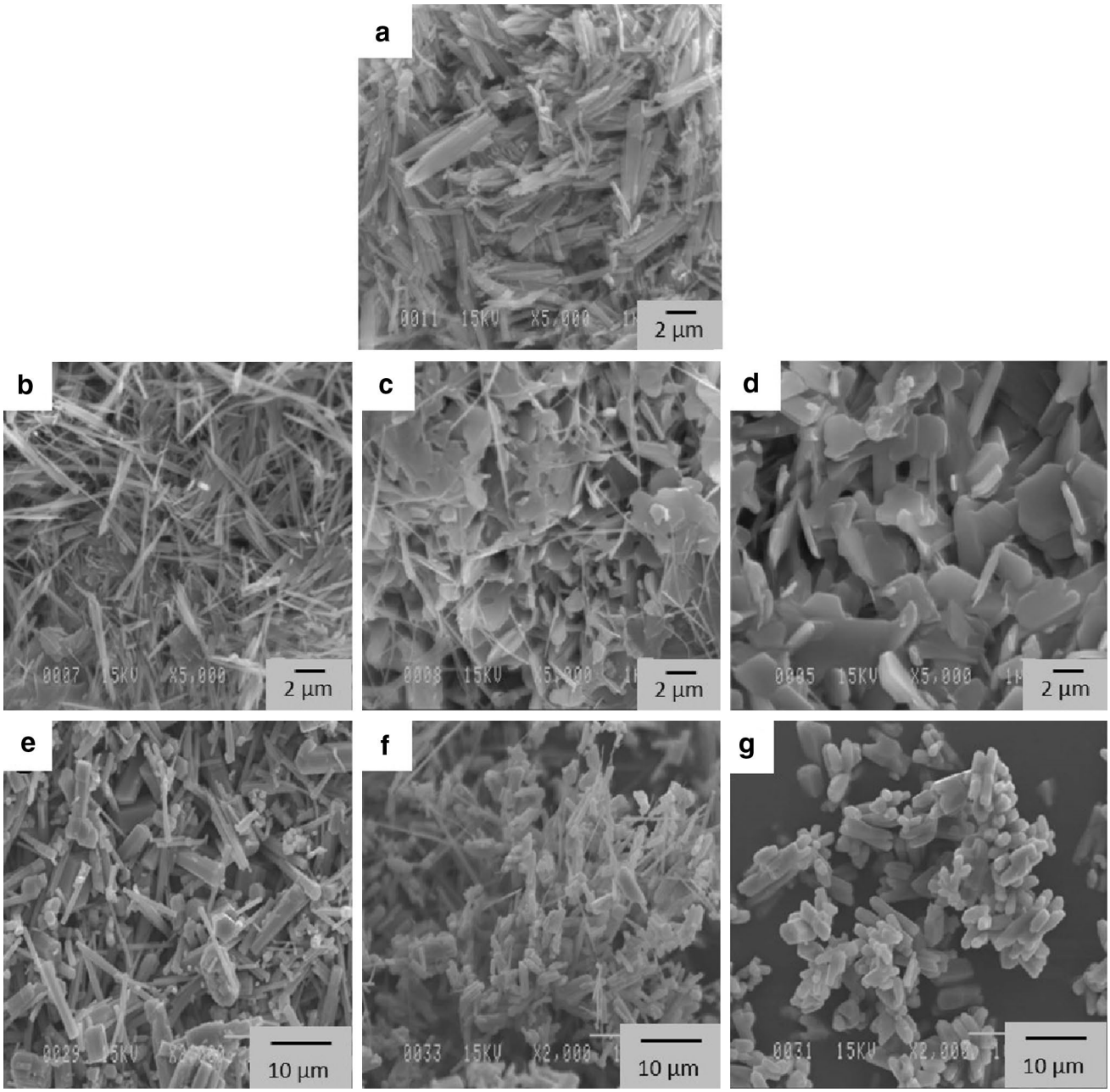

Fig. 2 SEM images of the synthesized molybdenum oxides: **a** MO, **b** MO–CTAB 1:4, **c** MO–CTAB 1:3, **d** MO–CTAB 1:2, **e** MO–TMAB 1:4, **f** MO–TMAB 1:3, and **g** MO–TMAB 1:2

the presence of TMAB (Figs. 3 and 4). The stretching mode of Mo=O bands was located at 965 and 934 cm^{-1} [29, 30], and no peak was observed around 995 cm^{-1}, which is generally assigned to stretching vibrations of Mo–O–Mo. It is a characteristic of the orthorhombic phase of MoO_3.

The peaks observed at 1630 and 3550 cm^{-1} were attributed to stretching and bending vibration of hydrogen bonded –OH groups, qualitatively confirming the presence of OH groups on the surface and water molecules adsorbed in the catalysts, which concur with the results of XRD analysis. Quantitative analysis of the water content of catalysts was performed by TGA.

Figures 5 and 6 show TGA curves of the samples synthesized with CTAB and TMAB, respectively. The TGA curve of MO (without surfactant; Figs. 5d or 6c) shows a primary weight loss (~12%) observed in the range of 70–200 °C, which corresponds to desorption of physically adsorbed water on MoO_3–H_2O. After 200 °C, the weight of MO remained constant up to 700 °C, confirming the thermal stability of molybdenum oxide without any surfactant

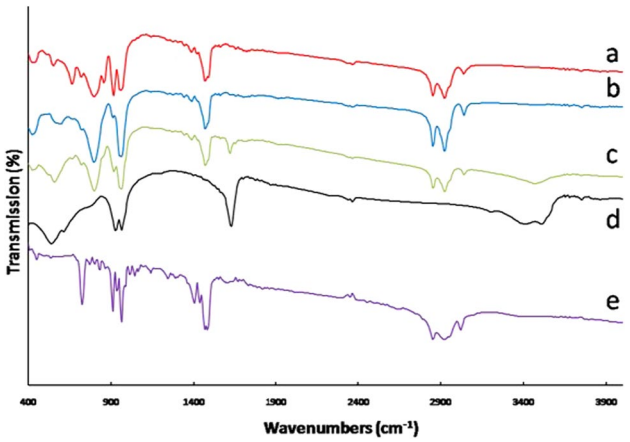

Fig. 3 FT-IR spectra of the molybdenum oxides prepared with CTAB at various concentrations: **a** MO–CTAB 1:2, **b** MO–CTAB 1:3, **c** MO–CTAB 1:4, **d** MO, and **e** CTAB

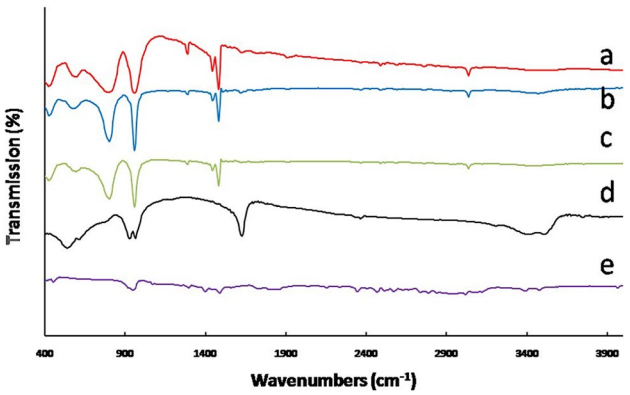

Fig. 4 FT-IR spectra of the molybdenum oxides prepared with TMAB at various concentrations: **a** MO–TMAB 1:2, **b** MO–TMAB 1:3, **c** MO–TMAB 1:4, **d** MO, and **e** TMAB

attached on its surface. Further heating after 700 °C led to a great weight loss, not only for the MO sample but also for the other samples, which is due to sublimation of molybdenum oxide that has been reported before [31].

TGA curves of the samples containing CTAB (Fig. 5a–c) generally show lower weight losses compared to MO in the low-temperature region of ˂200 °C, which was attributed to the hydrogen-bonded water molecules present in the crystalline phase; this assumption was confirmed by FT-IR analysis. The second weight loss observed at the range of 200–300 °C could be ascribed to decomposition of nitrates and ammonia compounds obtained from the surfactant. In addition, a third weight loss was obtained in the high-temperature region (300 ˂ T ˂ 500 °C), which further differential thermal analysis (DTA) confirmed that it belongs to an exothermic interaction. This weight loss could be ascribed to removal or decomposition of CTA^+ and elimination of bromide species during oxidation in air. The total amount of weight losses had a positive relationship with CTAB content in the samples; 50, 40, and 37% weight losses were obtained for MO–CTAB 1:2, 1:3, and 1:4, respectively. TGA curves of the samples with TMAB (Fig. 6) and their DTA analysis showed exothermic peaks between 300 and 450 °C, corresponding to elimination of $^{+}N(CH_3)_4$ group and bromide species. The weight losses during oxidation were between 16 and 17% which are much lower compared to those of the CTAB-capped samples. It could be due to the small molar weight of TMAB (210.16 g/mol) compared to that of CTAB (364.45 g/mol).

Catalytic Test Results

Catalytic activities of the surfactant-capped molybdenum oxide catalysts in oxidative scission of oleic acid were

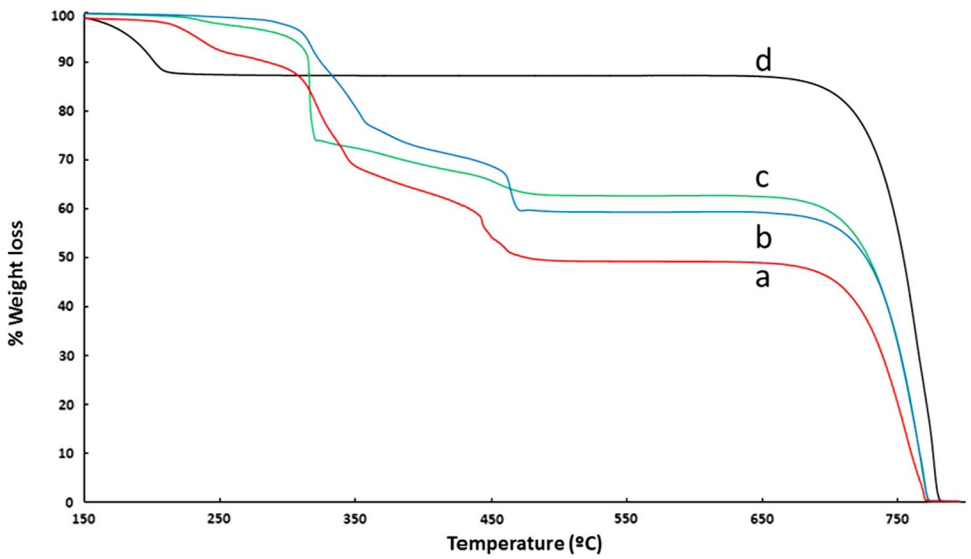

Fig. 5 TGA curves of the molybdenum oxides prepared with different amounts of CTAB: **a** MO–CTAB 1:2, **b** MO–CTAB 1:3, **c** MO–CTAB 1:4, and **d** MO

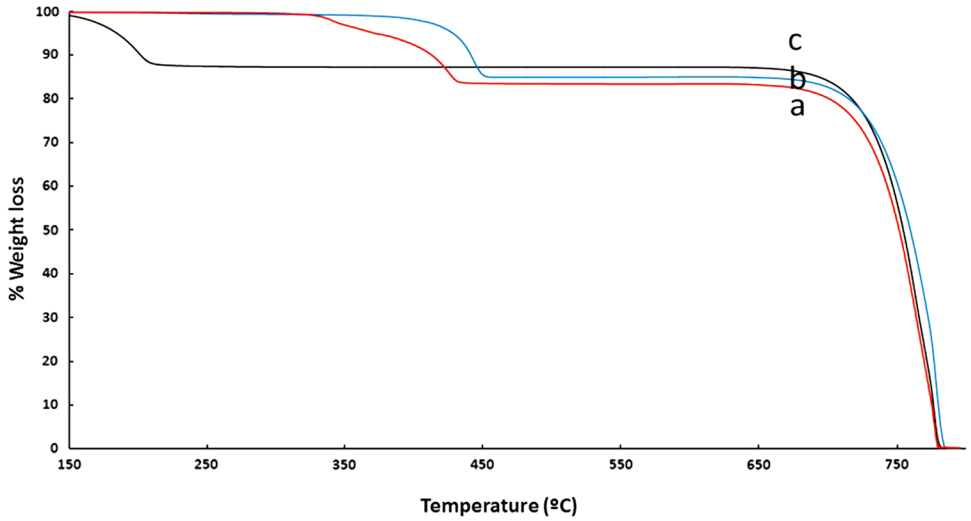

Fig. 6 TGA curves of the molybdenum oxides prepared with different amounts of TMAB: **a** MO–TMAB 1:2, **b** MO–TMAB 1:3, and **c** MO

investigated in a glass reactor equipped with condenser, thermocouple, and magnetic stirrer. A reaction was conducted without oleic acid to determine H_2O_2 loss via catalytic or thermal decomposition and the loss was calculated by titrimetry. For a 4-h reaction at 85 °C, the loss of the oxidant was 26%. Therefore, excess amounts of H_2O_2 were used to complete the oxidation reactions (the molar ratio of H_2O_2/oleic acid used in the reaction was 11.1, which shows an excess amount of H_2O_2 of about 180%, based on the stoichiometric reaction, Eq. 1).

The first step of the reaction involves protonation of a peroxo moiety on the catalyst to give surface peroxo groups. A yellow suspension was observed in the reaction solution, due to the formation of metal-peroxo complexes, –MoO(O_2), on surfaces of the surfactant-capped catalysts. Time-lapse observations of the reaction mixture containing catalyst, oleic acid, hydrogen peroxide, and *tert*-butanol was recorded during the reactions over the catalysts to track changes that take place slowly over time (Figure S1 and S2, Supporting Information). Intriguingly, the heterogeneity behavior of MO–CTAB 1:3 catalyst was changed during the reaction; in the beginning of the reaction, the catalyst was solid powders observable in the reaction mixture, which, upon heating to 85 °C, turned into a homogeneous system. Afterwards, the reaction mixture remined as a clear solution until the end of the reaction. As soon as the reaction mixture was cooled to room temperature, the catalyst started to precipitate (Figure S1), enabling self-separation and easy recovery of the catalyst. By contrast, all of the TMAB containing catalysts retained their solid and heterogeneous natures during the reaction (Figure S2). This may be due to the structural differences between these two surfactants; CTAB has a long hydrophobic chain of cetyl groups, which improves the hydrophobic–hydrophobic interaction between the surface of molybdenum oxide and oleic acid molecules and traps these molecules in the reaction medium, resulting in enhancement of contacts between the reactants and active sites on the catalyst. High dispersion of MO–CTAB 1:3 catalyst in the reaction mixture, which arose from the surface organo-modification, created conditions similar to homogeneous catalysis. Moreover, a high concentration of hydrogen peroxide during the reaction results in rapid formation of metal-peroxo complexes and reinforcement of the emulsion, while at the end of the reaction, when a majority of H_2O_2 has been consumed, concentration of such complexes on the catalyst's surface drops, resulting in precipitation of the catalyst.

Table 1 shows conversion of oleic acid and yields of production of the desired products, azelaic and pelargonic acids, over different synthesized catalysts with H_2O_2 as oxidant after 3.5 h of reaction at 85 °C. The catalytic test results presented are the average of at least three runs over each catalyst. The first catalytic test was done without any catalyst (Table 1, entry 1), that gives very low conversion (26%) and yields of azelaic and pelargonic acids (6.4 and 6.8%, respectively). Using the catalyst without surfactant, MO, significantly increased the conversion (97%) and yields of azelaic and pelargonic acids (60 and 50%, respectively; entry 2). An overwhelming majority of the organo-modified catalysts resulted in better efficiencies (entries 3–8). Ideally, oxidative cleavage of oleic acid should give similar yields of azelaic and pelargonic acids (1 mol of oleic acid into 1 mol of each product) based on the stoichiometric equation of the reaction (Eq. 1). In practice, however, differences were obtained in the yields of these two products, which arise from non-ideality of the catalytic system, different decomposition rates of azelaic and pelargonic acids in the reaction medium, and presence of by-products.

$$\begin{aligned} &H_3C(CH_2)_7CH \\ &\quad = CH(CH_2)_7COOH + 4H_2O_2 \xrightarrow{\text{Catalyst}} H_3C(CH_2)_7COOH \\ &\quad HOOC(CH_2)_7COOH + 4H_2O \end{aligned} \tag{1}$$

Table 1 Catalytic tests results (conversion of oleic acid and yields of production of desired products)

Entry	Catalyst	Surfactant:Mo molar ratio	Conversion[a] (%)	Yield[b] of azelaic acid (%)	Yield[b] of pelargonic acid (%)
1	Without catalyst	–	26	6.4	6.8
2	MO	0	97	60	50
3	MO–CTAB 1:4	1:4	100	78.2	61
4	MO–CTAB 1:3	1:3	100	83	68
5	MO–CTAB 1:2	1:2	100	70	55
6	MO–TMAB 1:4	1:4	100	68	59
7	MO–TMAB 1:3	1:3	100	67.4	60
8	MO–TMAB 1:2	1:2	100	58	46

[a] Reaction conditions: time: 3.5 h, temperature: 85 °C, solvent: *tert*-butanol, initial amounts of oleic acid: 1 g, *t*-butanol: 8 ml, H_2O_2: 4 ml, catalyst: 0.4 g

[b] Yield, in this work, is defined as the number of moles of a product formed per mole of oleic acid consumed

Use of the surfactants as capping agent increased yields of both azelaic and pelargonic acids. The maximum yields were achieved by MO–CTAB 1:3 catalyst (entry 4), which produced 83% azelaic and 68% pelargonic acids. Compared to the literature, these obtained yields are superior to what have been obtained by heterogeneous catalysts and are comparable with what homogeneous ones have shown. Table 2 lists the results of other works (all the heterogeneous catalysts reported so far, to the best of our knowledge, and some of the best homogeneous catalysts). The excellent catalytic activity of MO–CTAB 1:3, as Table 2 implies, could be ascribed to the presence of multiple alkyl chains on the catalyst's surface, which improve the interactions of oleic acid with peroxo-molybdenum complexes formed by the reaction of H_2O_2 with the particles' surfaces.

Recyclability of the Catalysts

Stability and, consequently, reusability of the catalyst, which are important parameters to scale up the process, were also investigated for the catalyst that gave the best efficiency (MO–CTAB 1:3). The catalyst was conveniently recovered from the mixture of products after the reaction by simple centrifugation at high rpm. No significant loss of catalyst (or no significant leaching of Mo species to the reaction solution) was found, even after four cycles of catalytic reaction. Yield of weight recovery for all the catalysts after the first cycle was more than ~97% and loss of the CTAB-capped catalyst after four cycles obtained by ICP analysis was 9.4 wt%. This good recovery could be due to the protective role of the capping surfactant on the catalyst surface. Table 3 represents catalytic efficiencies obtained by catalyst MO–CTAB 1:3 in the four performed reaction cycles, which shows insignificant activity loss. Yields of desired products slightly decreased during the cycles while the conversion was always the same. Comparing FT-IR spectra of MO–CTAB 1:3 before and after each cycle (Fig. 7) does not show any notable difference, which proves the stability of the CTAB capped on the catalyst's surface. Even after the fourth cycle, CTAB groups were still attached to the catalyst; all the characteristic peaks of the alkyl group and molybdenum oxide remained after the cycles. The slight decrease in the yields may be due to the progressive detachment of CTAB and leaching of molybdenum oxide from the particle surface to the solution (leaching of Mo oxide: ~10% after 4 cycles of reaction). Furthermore, to verify that the reaction is truly heterogeneous and to investigate the possibility of leaching of Mo species in the reaction solution after removal of the catalyst, a catalytic test was performed with MoCTAB 1:3 catalyst and stopped after 1 h of reaction, which showed 44% conversion and 28 and 21% yields of azelaic and pelargonic acids, respectively. After cooling to room temperature, the catalyst was removed, and the reaction solution was exposed to the reaction conditions for the remaining reaction time (2.5 h, at 85 °C). Although the conversion increased to 61%, the yields were negligibly changed (29 and 23% for azelaic and pelargonic acids, respectively), which could be well ascribed to the lack of catalyst. However, since the oxidant could cause the conversion of oleic acid independently (see Table 1, entry 1), the conversion was increased somewhat. From these results, it can be concluded that this new catalytic system displays high activity, good selectivity, and environmentally benign properties (using hydrogen peroxide instead of hazardous ozone) and the efficient reusability of the catalyst makes the process cost-effective and eco-friendly.

Conclusions

In summary, we have reported successful synthesis of surfactant-capped molybdenum oxide catalysts by a simple

Table 2 Comparison of catalytic efficiency of MO–CTAB 1:3 with recent reported works in the literature

Catalyst/oxidant system	Reaction time and temperature	Conversion (%)	Yield[a] (%)	References
Peroxo-tungsten complex PTA/H_2O_2	5 h, 80 °C	–	PA: 82 AA: 79	[2][b]
Polyoxomolybdate	5 h, 90 °C	–	AA: 82	[6][b]
$RuCl_3/NaIO_4$	8 h, RT	–	PA: 98 AA: 62	[11][b]
H_2WO_4/H_2O_2	8 h, 100 °C	–	PA: 69 AA: 92	[17][b]
Tungsten oxide-SiO_2/H_2O_2	1 h, 130 °C	79	PA: 36 AA: 32	[32][c]
Tungsten oxide/H_2O_2	1 h, 130 °C	56	PA: 29 AA: 30	[32][c]
Chromium supported on MCM-41/O_2	8 h, 80 °C	>95	AA: 32.4 PA: 32.2	[9][c]
Tungsten oxide/H_2O_2	5 h, 120 °C	95	AA: 58 PA: 24	[33][c]
H_2O_2/MO–CTAB 1:3	3.5 h, 85 °C	100	PA: 68% AA: 83%	This work[c]

[a] *AA* azelaic acid, *PA* pelargonic acid

[b] Homogeneous catalysis

[c] Heterogeneous catalysis

Table 3 Catalytic efficiencies obtained by catalyst MO–CTAB 1:3 in different reaction cycles

Catalysts	Reaction cycle	Conversion[a] (%)	Yield[b] of azelaic acid (%)	Yield[b] of pelargonic acid (%)
MO–CTAB 1:3	1	100	83	68
MO–CTAB 1:3	2	100	80	65
MO–CTAB 1:3	3	100	78	63
MO–CTAB 1:3	4	99	77	61

[a] Reaction conditions: time: 3.5 h, temperature: 85 °C, solvent: *tert*-butanol, initial amounts of oleic acid: 1 g, *t*-butanol: 8 ml, H_2O_2: 4 ml, catalyst: 0.4 g

[b] Yield, in this work, is defined as the number of moles of a product formed per mole of oleic acid consumed

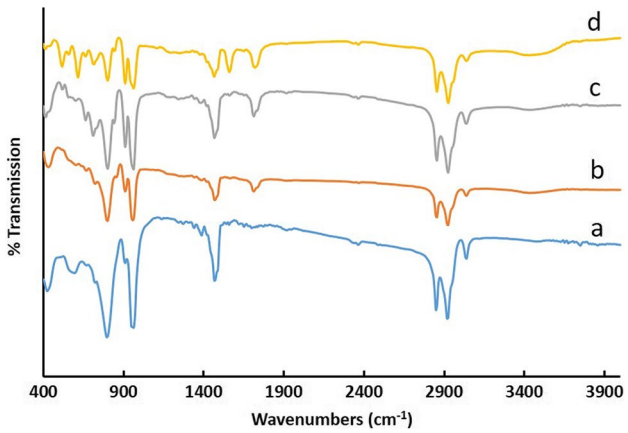

Fig. 7 FT-IR spectra of MO–CTAB 1:3 catalyst after different reaction cycles: **a** after cycle 1, **b** after cycle 2, **c** after cycle 3, and **d** after cycle 4

oxidative dissolution method at 100 °C, which were characterized by different techniques including XRD, FT-IR, TGA, and SEM analyses. CTAB and TMAB were used as surfactants to organo-modify surfaces of the molybdenum oxides. The physicochemical analysis revealed that morphology of the products strongly depends on nature and concentration of capping agents. The synthesized surfactant-capped catalysts showed excellent catalytic efficiency in oxidative cleavage of oleic acid to mono- and dicarboxylic acids. The highest efficiency was obtained for the CTAB-capped molybdenum oxide (with CTAB/Mo molar ratio of 1/3), resulting in full conversion of oleic acid and 83 and 68% yields of production of azelaic and pelargonic acids, respectively. This catalyst exhibited convenient recovery, good stability, and steady reusability over recycling experiments without significant activity loss up to four cycles. Employing an environmentally benign oxidant, hydrogen peroxide, this catalytic system would open a new pathway for production of diacids and fuel components from renewable feedstock.

Acknowledgements ASE thanks the Department of Chemical Engineering at Laval University for welcoming him as a visiting scientist during his stay in Canada. The authors would like to thank the industrial partners (Oleotek and SiliCycle Inc.) for stimulating discussions and comments.

Compliance with Ethical Standards

Conflict of interest The authors declare that they have no conflicts of interest.

Funding This study was funded by the "Programme Canadien de Bourses de la Francophonie" (PCBF) and the Nature Sciences and Engineering Research Council of Canada (NSERC) through an INNOV-UC grant.

References

1. Rhead MM, Eglinton G, Draffan GH, England PJ (1971) Conversion of oleic acid to saturated fatty acids in Severn estuary sediments. Nature 232(5309):327–330
2. Godard A, De Caro P, Thiebaud-Roux S, Vedrenne E, Mouloungui Z (2013) New environmentally friendly oxidative scission of oleic acid into azelaic acid and pelargonic acid. J Am Oil Chem Soc 90(1):133–140. doi:10.1007/s11746-012-2134-7
3. Köckritz A, Blumenstein M, Martin A (2010) Catalytic cleavage of methyl oleate or oleic acid. Eur J Lipid Sci Technol 112(1):58–63. doi:10.1002/ejlt.200900103
4. Kulik A, Janz A, Pohl M-M, Martin A, Köckritz A (2012) Gold-catalyzed synthesis of dicarboxylic and monocarboxylic acids. Eur J Lipid Sci Technol 114(11):1327–1332. doi:10.1002/ejlt.201200027
5. Noureddini H, Rempe ML (1996) Pelargonic acid in enhanced oil recovery. J Am Oil Chem Soc 73(7):939–941. doi:10.1007/bf02517999
6. Turnwald SE, Lorier MA, Wright LJ, Mucalo MR (1998) Oleic acid oxidation using hydrogen peroxide in conjunction with transition metal catalysis. J Mater Sci Lett 17(15):1305–1307. doi:10.1023/a:1006532314593
7. Enferadi Kerenkan A, Beland F, Do T-O (2016) Chemically catalyzed oxidative cleavage of unsaturated fatty acids and their derivatives into valuable products for industrial applications: a review and perspective. Catal Sci Technol 6(4):971–987. doi:10.1039/C5CY01118C
8. Spannring P, Bruijnincx PCA, Weckhuysen BM, Klein Gebbink RJM (2014) Transition metal-catalyzed oxidative double bond cleavage of simple and bio-derived alkenes and unsaturated fatty acids. Catal Sci Technol 4(8):2182–2209. doi:10.1039/C3CY01095C
9. Dapurkar SE, Kawanami H, Yokoyama T, Ikushima Y (2009) Catalytic oxidation of oleic acid in supercritical carbon dioxide media with molecular oxygen. Top Catal 52(6):707–713. doi:10.1007/s11244-009-9212-6
10. Sparks DL, Antonio Estevez L, Hernandez R (2009) Supercritical-fluid-assisted oxidation of oleic acid with ozone and potassium permanganate. Green Chem 11(7):986–993. doi:10.1039/B816515G
11. Rup S, Sindt M, Oget N (2010) Catalytic oxidative cleavage of olefins by RuO_4 organic solvent-free under ultrasonic irradiation. Tetrahedron Lett 51(23):3123–3126. doi:10.1016/j.tetlet.2010.04.040
12. Rup S, Zimmermann F, Meux E, Schneider M, Sindt M, Oget N (2009) The ultrasound-assisted oxidative scission of monoenic fatty acids by ruthenium tetroxide catalysis: influence of the mixture of solvents. Ultrason Sonochem 16(2):266–272. doi:10.1016/j.ultsonch.2008.08.003
13. Dai B, Wu P, Zhu W, Chao Y, Sun J, Xiong J, Jiang W, Li H (2016) Heterogenization of homogenous oxidative desulfurization reaction on graphene-like boron nitride with a peroxomolybdate ionic liquid. RSC Adv 6(1):140–147. doi:10.1039/C5RA23272D
14. Du D-Y, Qin J-S, Li S-L, Su Z-M, Lan Y-Q (2014) Recent advances in porous polyoxometalate-based metal-organic framework materials. Chem Soc Rev 43(13):4615–4632. doi:10.1039/C3CS60404G
15. Song Y-F, Tsunashima R (2012) Recent advances on polyoxometalate-based molecular and composite materials. Chem Soc Rev 41(22):7384–7402. doi:10.1039/C2CS35143A
16. Zhou Y, Chen G, Long Z, Wang J (2014) Recent advances in polyoxometalate-based heterogeneous catalytic materials for liquid-phase organic transformations. RSC Adv 4(79):42092–42113. doi:10.1039/C4RA05175K
17. Benessere V, Cucciolito ME, De Santis A, Di Serio M, Esposito R, Ruffo F, Turco R (2015) Sustainable process for production of azelaic acid through oxidative cleavage of oleic acid. J Am Oil Chem Soc 92(11):1701–1707. doi:10.1007/s11746-015-2727-z
18. Chandra P, Doke DS, Umbarkar SB, Biradar AV (2014) One-pot synthesis of ultrasmall MoO_3 nanoparticles supported on SiO_2, TiO_2, and ZrO_2 nanospheres: an efficient epoxidation catalyst. J Mater Chem A 2(44):19060–19066. doi:10.1039/C4TA03754E
19. Li Z, Li Y, Zhan E, Ta N, Shen W (2013) Morphology-controlled synthesis of [small alpha]-MoO_3 nanomaterials for ethanol oxidation. J Mater Chem A 1(48):15370–15376. doi:10.1039/C3TA13402D
20. Ma Z, Wu Y, He Y, Wu T (2013) A novel protocol for the oxidative degradation of chitosan with hydrogen peroxide catalyzed by peroxomolybdate in aqueous solution. RSC Adv 3(30):12049–12051. doi:10.1039/C3RA40424B
21. Metcalfe LD, Schmitz AA (1961) The rapid preparation of fatty acid esters for gas chromatographic analysis. Anal Chem 33(3):363–364. doi:10.1021/ac60171a016
22. Metcalfe LD, Schmitz AA, Pelka JR (1966) Rapid preparation of fatty acid esters from lipids for gas chromatographic analysis. Anal Chem 38(3):514–515. doi:10.1021/ac60235a044
23. Song R-Q, Xu A-W, Deng B, Fang Y-P (2005) Novel multilamellar mesostructured molybdenum oxide nanofibers and nanobelts: synthesis and characterization. J Phys Chem B 109(48):22758–22766. doi:10.1021/jp0533325
24. Wang S, Zhang Y, Ma X, Wang W, Li X, Zhang Z, Qian Y (2005) Hydrothermal route to single crystalline α-MoO_3 nanobelts and hierarchical structures. Solid State Commun 136(5):283–287. doi:10.1016/j.ssc.2005.08.002
25. Gong J, Zeng W, Zhang H (2015) Hydrothermal synthesis of controlled morphologies of MoO_3 nanobelts and hierarchical structures. Mater Lett 154:170–172. doi:10.1016/j.matlet.2015.04.092
26. Li Y, Liu T, Li T, Peng X (2015) Hydrothermal fabrication of controlled morphologies of MoO_3 with CTAB: structure and growth. Mater Lett 140:48–50. doi:10.1016/j.matlet.2014.10.153
27. Chithambararaj A, Chandra Bose A (2014) Role of synthesis variables on controlled nucleation and growth of hexagonal molybdenum oxide nanocrystals: investigation on thermal and optical properties. CrystEngComm 16(27):6175–6186. doi:10.1039/C4CE00418C
28. Chithambararaj A, Sanjini NS, Bose AC, Velmathi S (2013) Flower-like hierarchical h-MoO_3: new findings of efficient visible light driven nano photocatalyst for methylene blue degradation. Catal Sci Technol 3(5):1405–1414. doi:10.1039/C3CY20764A
29. Chithambararaj A, Bose AC (2011) Hydrothermal synthesis of hexagonal and orthorhombic MoO_3 nanoparticles. J Alloy Compd 509(31):8105–8110. doi:10.1016/j.jallcom.2011.05.067
30. Masteri-Farahani M, Mahdavi S, Rafizadeh M (2013) Microemulsion-mediated synthesis and characterization of monodispersed nickel molybdate nanocrystals. Ceram Int 39(4):4619–4625. doi:10.1016/j.ceramint.2012.11.059

31. Mao Y, Li W, Sun X, Ma Y, Xia J, Zhao Y, Lu X, Gan J, Liu Z, Chen J, Liu P, Tong Y (2012) Room-temperature ferromagnetism in hierarchically branched MoO_3 nanostructures. CrystEngComm 14(4):1419–1424. doi:10.1039/C1CE05700F
32. Noureddini H, Kanabur M (1999) Liquid-phase catalytic oxidation of unsaturated fatty acids. J Am Oil Chem Soc 76(3):305–312. doi:10.1007/s11746-999-0236-7
33. Enferadi Kerenkan A, Ello Aimé S, Echchahed B, Do T-O (2016) Synthesis of mesoporous tungsten oxide/γ-alumina and surfactant-capped tungsten oxide nanoparticles and their catalytic activities in oxidative cleavage of oleic acid. Int J Chem Reactor Eng 14(4):899–907